

Dark $SU(2) \rightarrow Z_3 \times Z_2$ Gauge Symmetry

Debasish Borah

Department of Physics, Indian Institute of Technology Guwahati, Assam 781039, India

Ernest Ma

*Department of Physics and Astronomy,
University of California, Riverside, California 92521, USA*

Dibyendu Nanda

School of Physics, Korea Institute for Advanced Study, Seoul 02455, Korea

Abstract

The dark sector is postulated to be invariant under an $SU(2)$ gauge symmetry, spontaneously broken by a Higgs quadruplet to a conserved residual $Z_3 \times Z_2$ symmetry. The resulting dark matter phenomenology is studied.

I. INTRODUCTION

Whereas the stability of dark matter (DM) [1] is most likely due to an unbroken symmetry [2, 3], its nature and its origin are both unknown. It may well have something to do with a non-Abelian gauge symmetry, the simplest of which is $SU(2)$ [4]. The associated gauge bosons are presumably heavy from the spontaneous breaking of the gauge symmetry through Higgs scalars. If a Higgs doublet is used, then the resulting theory has a residual $SU(2)$ global symmetry [4, 5]. If both a doublet and a triplet are used, then the breaking may be gauge $SU(2)$ to gauge $U(1)$ to global $U(1)$ [6]. If other scalar multiplets are used, there are various possible outcomes [7]. In this paper, we study in detail the case of a Higgs $SU(2)$ quadruplet [8], resulting in a dark discrete Z_3 symmetry [9–11]. We show that an extra Z_2 symmetry emerges as the result of the structure of this particular scalar potential, which was not recognized previously. We identify the possible dark matter candidates and study their phenomenology in relic abundance and direct detection. We note that the idea of gauge $SU(2)$ family symmetry breaking to A_4 using a Higgs septuplet has also been studied [12].

II. THE MODEL

Consider the origin of dark matter as coming from an $SU(2)$ gauge symmetry, broken by a Higgs quadruplet Φ . The complete scalar potential involving Φ is given by

$$V = -\mu^2 \Phi^\dagger \Phi + \frac{1}{2} \lambda_1 (\Phi^\dagger \Phi)^2 - \frac{10}{9} \lambda_2 (\Phi \tilde{\Phi})_3 (\Phi \tilde{\Phi})_3 - \left[\frac{5}{18} \lambda_3 (\Phi \Phi)_3 (\Phi \Phi)_3 + \frac{5}{9} \lambda_4 (\Phi \Phi)_3 (\Phi \tilde{\Phi})_3 + \text{h.c.} \right]. \quad (1)$$

To justify the above, let $\Phi = (\phi_3, \phi_2, \phi_1, \phi_0)$, then the only quadratic invariant is $\Phi^\dagger \Phi$. Now $(\Phi\Phi)_1 = (\Phi\Phi)_5 = 0$, whereas

$$(\Phi\Phi)_3 = \begin{pmatrix} \sqrt{\frac{3}{10}}\phi_3\phi_1 - \sqrt{\frac{2}{5}}\phi_2\phi_2 + \sqrt{\frac{3}{10}}\phi_1\phi_3 \\ \sqrt{\frac{9}{20}}\phi_3\phi_0 - \sqrt{\frac{1}{20}}\phi_2\phi_1 - \sqrt{\frac{1}{20}}\phi_1\phi_2 + \sqrt{\frac{9}{20}}\phi_0\phi_3 \\ \sqrt{\frac{3}{10}}\phi_2\phi_0 - \sqrt{\frac{2}{5}}\phi_1\phi_1 + \sqrt{\frac{3}{10}}\phi_0\phi_2 \end{pmatrix}, \quad (2)$$

and

$$(\Phi\Phi)_3(\Phi\Phi)_3 = \frac{3}{5}(6\phi_0\phi_1\phi_2\phi_3 - 3\phi_0^2\phi_3^2 + \phi_1^2\phi_2^2) - \frac{4\sqrt{3}}{5}(\phi_0\phi_2^3 + \phi_1^3\phi_3). \quad (3)$$

As for $(\Phi\Phi)_7$, it may be neglected because $(\Phi\Phi)_7(\Phi\Phi)_7 = -(\Phi\Phi)_3(\Phi\Phi)_3$.

Consider now $\tilde{\Phi} = (\phi_0^*, -\phi_1^*, \phi_2^*, -\phi_3^*)$, which transforms as Φ .

$$(\Phi\tilde{\Phi})_3 = \begin{pmatrix} \sqrt{\frac{3}{10}}\phi_3\phi_2^* + \sqrt{\frac{2}{5}}\phi_2\phi_1^* + \sqrt{\frac{3}{10}}\phi_1\phi_0^* \\ -\sqrt{\frac{9}{20}}\phi_3\phi_3^* - \sqrt{\frac{1}{20}}\phi_2\phi_2^* + \sqrt{\frac{1}{20}}\phi_1\phi_1^* + \sqrt{\frac{9}{20}}\phi_0\phi_0^* \\ -\sqrt{\frac{3}{10}}\phi_2\phi_3^* - \sqrt{\frac{2}{5}}\phi_1\phi_2^* - \sqrt{\frac{3}{10}}\phi_0\phi_1^* \end{pmatrix}. \quad (4)$$

Hence

$$(\Phi\tilde{\Phi})_3(\Phi\tilde{\Phi})_3 = -\frac{1}{20}(3|\phi_0|^2 + |\phi_1|^2 - |\phi_2|^2 - 3|\phi_3|^2)^2 - \frac{1}{5}|\sqrt{3}\phi_0\phi_1^* + 2\phi_1\phi_2^* + \sqrt{3}\phi_2\phi_3^*|^2, \quad (5)$$

which is the same as $-(\Phi^\dagger\Phi)_3(\Phi^\dagger\Phi)_3$.

Finally,

$$\begin{aligned} (\Phi\Phi)_3(\Phi\tilde{\Phi})_3 &= \frac{9}{10}(\phi_1\phi_2 - \phi_0\phi_3)(|\phi_0|^2 - |\phi_3|^2) + \frac{3}{10}(\phi_1\phi_2 + 3\phi_0\phi_3)(|\phi_2|^2 - |\phi_1|^2) \\ &+ \frac{\sqrt{3}}{5}(\phi_2\phi_2\phi_2\phi_3^* - \phi_0^*\phi_1\phi_1\phi_1 + 3\phi_0\phi_1^*\phi_2\phi_2 - 3\phi_1\phi_1\phi_2^*\phi_3), \end{aligned} \quad (6)$$

which is the same as $-(\Phi\Phi)_7(\Phi\tilde{\Phi})_7$.

As ϕ_0 and ϕ_3 develop vacuum expectation values, a residual Z_3 symmetry remains, maintained by $\phi_1 \sim \omega$, $\phi_2 \sim \omega^2$, with $\phi_{0,3} \sim 1$, where $\omega^3 = 1$.

Let $\langle\phi_{0,3}\rangle = v_{0,3}$, then V is minimized with

$$0 = v_0[-\mu^2 + \lambda_1(v_0^2 + v_3^2) + \lambda_2(v_0^2 - v_3^2) + \lambda_3v_3^2 + (3/2)\lambda_4v_0v_3] - \lambda_4v_3^3/2, \quad (7)$$

$$0 = v_3[-\mu^2 + \lambda_1(v_0^2 + v_3^2) + \lambda_2(v_3^2 - v_0^2) + \lambda_3v_0^2 - (3/2)\lambda_4v_0v_3] + \lambda_4v_0^3/2. \quad (8)$$

Let $v_D = \sqrt{v_0^2 + v_3^2}$, $c = \cos \theta = v_0/v_D$, $s = \sin \theta = v_3/v_D$, then

$$\frac{\lambda_4}{2\lambda_2 - \lambda_3} = \frac{2sc(c^2 - s^2)}{c^4 + s^4 - 6s^2c^2} = \frac{1}{2} \tan 4\theta, \quad (9)$$

$$v_D^2 = \frac{2\mu^2}{2\lambda_1 + \lambda_3 + (\tan 4\theta/2 \tan 2\theta)(2\lambda_2 - \lambda_3)}. \quad (10)$$

The scalar masses and interactions are then functions of v_D , θ , and $\lambda_{1,2,3}$.

It is worth mentioning that the authors of [8] have already shown that breaking $SU(2)$ symmetry with a quadruplet always leads to remnant Z_3 symmetry. In other words, it is always possible to redefine the $SU(2)$ basis to make $\langle \phi_1 \rangle = v_1 = 0$, $\langle \phi_2 \rangle = v_2 = 0$, as chosen above. However, we have discovered that an extra accidental Z_2 symmetry appears from its detailed structure.

A. Dark Sector Mass Spectrum and Interactions

The dark gauge bosons $X_{1,2,3}$ interact with Φ according to

$$\left| \partial \begin{pmatrix} \phi_3 \\ \phi_2 \\ \phi_1 \\ \phi_0 \end{pmatrix} - ig_D \begin{pmatrix} \frac{3}{2}X_3 & \frac{\sqrt{3}}{2}(X_1 - iX_2) & 0 & 0 \\ \frac{\sqrt{3}}{2}(X_1 + iX_2) & \frac{1}{2}X_3 & X_1 - iX_2 & 0 \\ 0 & X_1 + iX_2 & -\frac{1}{2}X_3 & \frac{\sqrt{3}}{2}(X_1 - iX_2) \\ 0 & 0 & \frac{\sqrt{3}}{2}(X_1 + iX_2) & -\frac{3}{2}X_3 \end{pmatrix} \begin{pmatrix} \phi_3 \\ \phi_2 \\ \phi_1 \\ \phi_0 \end{pmatrix} \right|^2. \quad (11)$$

The masses of $X_{1,2,3}$ are

$$M_{1,2}^2 = \frac{3}{2}g_D^2v_D^2, \quad M_3^2 = \frac{9}{2}g_D^2v_D^2, \quad (12)$$

with $c\phi_1 - s\phi_2^*$ and $\sqrt{2}\text{Im}(c\phi_0 - s\phi_3)$ as the longitudinal components of $(X_1 - iX_2)/\sqrt{2} \sim \omega$ and $X_3 \sim 1$ respectively under Z_3 . The orthogonal components $\eta = s\phi_1 + c\phi_2^*$ and $\phi_I = \sqrt{2}\text{Im}(s\phi_0 + c\phi_3)$ have masses

$$M_\eta^2 = \frac{2}{3}\lambda_2v_D^2 + \frac{1}{2}M_{\phi_I}^2, \quad M_{\phi_I}^2 = - \left[2\lambda_3 + \frac{\tan 4\theta}{\tan 2\theta}(2\lambda_2 - \lambda_3) \right] v_D^2. \quad (13)$$

The 2×2 mass-squared matrix spanning $\sqrt{2}\text{Re}(\phi_0, \phi_3)$ is

$$M_R^2 = \begin{pmatrix} 2(\lambda_1 + \lambda_2)c^2 + (1/2)\lambda_4(3sc + s^3/c) & 2(\lambda_1 - \lambda_2 + \lambda_3)sc + (3/2)\lambda_4(c^2 - s^2) \\ 2(\lambda_1 - \lambda_2 + \lambda_3)sc + (3/2)\lambda_4(c^2 - s^2) & 2(\lambda_1 + \lambda_2)s^2 - (1/2)\lambda_4(3sc + c^3/s) \end{pmatrix} v_D^2. \quad (14)$$

Let $\zeta = \sqrt{2}\text{Re}(c\phi_0 + s\phi_3)$ and $\phi_R = \sqrt{2}\text{Re}(s\phi_0 - c\phi_3)$, then they are mass eigenstates, using the identity of Eq. (9), with masses

$$M_\zeta^2 = [2\lambda_1 + \lambda_3 + \frac{\cos^2 2\theta}{\cos 4\theta}(2\lambda_2 - \lambda_3)]v_D^2, \quad (15)$$

$$M_{\phi_R}^2 = \frac{-1}{\cos 4\theta}(2\lambda_2 - \lambda_3)v_D^2. \quad (16)$$

Hence $\langle \zeta \rangle = \sqrt{2}v$ and $\langle \phi_R \rangle = 0$, with the latter (but not the former) connected to ϕ_I through X_3 . This has the important consequence of the emergence of an extra Z_2 symmetry, under which $\phi_{R,I}$ are odd and ζ, η are even. As for the dark gauge bosons, $X_1 \pm iX_2$ are odd and X_3 is even.

The physical scalars are now contained in $\phi_{0,1,2,3}$ as follows.

$$\phi_0 \rightarrow cv_D + \frac{1}{\sqrt{2}}(c\zeta + s\phi_R) + \frac{is}{\sqrt{2}}\phi_I, \quad (17)$$

$$\phi_1 \rightarrow s\eta, \quad \phi_2 \rightarrow c\eta^*, \quad (18)$$

$$\phi_3 \rightarrow sv_D + \frac{1}{\sqrt{2}}(s\zeta - c\phi_R) + \frac{ic}{\sqrt{2}}\phi_I. \quad (19)$$

The gauge-scalar interactions are

$$\begin{aligned}
\mathcal{L}_{int}^{gs} = & \frac{3}{4}g_D X_3(\phi_R \partial \phi_I - \phi_I \partial \phi_R) + \frac{i}{2}g_D X_3(\eta \partial \eta^* - \eta^* \partial \eta) \\
& + \frac{\sqrt{3}}{2}ig_D \left[\frac{X_1 + iX_2}{\sqrt{2}}(\phi_R - i\phi_I)\partial\eta - \frac{X_1 - iX_2}{\sqrt{2}}(\phi_R + i\phi_I)\partial\eta^* \right] \\
& - \frac{\sqrt{3}}{2}ig_D \left[\frac{X_1 + iX_2}{\sqrt{2}}\eta\partial(\phi_R - i\phi_I) - \frac{X_1 - iX_2}{\sqrt{2}}\eta^*\partial(\phi_R + i\phi_I) \right] \\
& + \frac{3}{8}g_D^2(3X_3^2 + X_1^2 + X_2^2)(2\sqrt{2}v_D\zeta + \zeta^2 + \phi_R^2 + \phi_I^2) + \frac{1}{4}g_D^2(X_3^2 + 7X_1^2 + 7X_2^2)|\eta|^2 \\
& - \sqrt{3}g_D^2 X_3 \left(\frac{X_1 + iX_2}{\sqrt{2}} \right) (\phi_R - i\phi_I)\eta - \sqrt{3}g_D^2 X_3 \left(\frac{X_1 - iX_2}{\sqrt{2}} \right) (\phi_R + i\phi_I)\eta^* \\
& + \sqrt{\frac{3}{2}}g_D^2(\sqrt{2}v_D + \zeta) \left[\left(\frac{X_1 - iX_2}{\sqrt{2}} \right)^2 \eta + \left(\frac{X_1 + iX_2}{\sqrt{2}} \right)^2 \eta^* \right]. \tag{20}
\end{aligned}$$

Let $x = \sin^2 2\theta$, then

$$M_{\phi_R}^2 = \frac{1}{2x-1}(2\lambda_2 - \lambda_3)v_D^2, \tag{21}$$

$$M_{\phi_I}^2 = -(2\lambda_2 + \lambda_3)v_D^2 + M_{\phi_R}^2, \tag{22}$$

$$M_\eta^2 = \frac{2}{3}\lambda_2 v_D^2 + \frac{1}{2}M_{\phi_I}^2, \tag{23}$$

$$M_\zeta^2 = 2\lambda_1 v_D^2 - \frac{1}{2}M_{\phi_I}^2 = 2\lambda_D v_D^2. \tag{24}$$

Inverting the above,

$$\lambda_1 v_D^2 = \frac{1}{2}M_\zeta^2 + \frac{1}{4}M_{\phi_I}^2, \tag{25}$$

$$\lambda_2 v_D^2 = \frac{3}{2}M_\eta^2 - \frac{3}{4}M_{\phi_I}^2, \tag{26}$$

$$\lambda_3 v_D^2 = M_{\phi_R}^2 + \frac{1}{2}M_{\phi_I}^2 - 3M_\eta^2, \tag{27}$$

$$xM_{\phi_R}^2 = 3M_\eta^2 - M_{\phi_I}^2. \tag{28}$$

B. Dark Sector Interactions with the Standard Model

With the addition of the Standard Model (SM) Higgs doublet H which is a singlet under the dark gauge $SU(2)$, the complete scalar interactions are then given by

$$\begin{aligned}
-\mathcal{L}_{int} = & \frac{M_\zeta^2}{2v_D^2} \left[\frac{v_D \zeta^3}{\sqrt{2}} + \frac{1}{8} \zeta^4 + \frac{1}{8} (\phi_R^2 + \phi_I^2)(\phi_R^2 + \phi_I^2 + 4|\eta|^2) \right] + \left(\frac{M_\zeta^2}{2v_D^2} + \frac{M_{\phi_R}^2}{v_D^2} \right) \left[\frac{v_D \zeta}{\sqrt{2}} + \frac{1}{4} \zeta^2 \right] \phi_R^2 \\
& + \left(\frac{M_\zeta^2}{2v_D^2} + \frac{M_\eta^2}{v_D^2} \right) \left[\frac{v_D \zeta}{\sqrt{2}} + \frac{1}{4} \zeta^2 \right] |\eta|^2 + \left(\frac{M_\zeta^2}{2v_D^2} + \frac{3M_\eta^2}{v_D^2} - \frac{M_{\phi_R}^2}{v_D^2} \right) \left[\frac{v_D \zeta}{\sqrt{2}} + \frac{1}{4} \zeta^2 \right] \phi_I^2 \\
& + \left(\frac{M_\zeta^2}{4v_D^2} + \frac{M_\eta^2}{3v_D^2} \right) |\eta|^4 + \frac{1}{3\sqrt{3}} \left(\frac{2M_{\phi_R}^2}{v_D^2} - \frac{3M_\eta^2}{v_D^2} \right) \left[v_D + \frac{\zeta}{\sqrt{2}} \right] (\eta^3 + \eta^{*3}) \\
& + \lambda_{H\phi} (H^\dagger H) (\Phi^\dagger \Phi) - \mu_H^2 (H^\dagger H) + \frac{\lambda_H}{2} (H^\dagger H)^2,
\end{aligned} \tag{29}$$

where

$$(H^\dagger H) = \left(v_H + \frac{h}{\sqrt{2}} \right)^2, \tag{30}$$

$$(\Phi^\dagger \Phi) = \left(v_D + \frac{\zeta}{\sqrt{2}} \right)^2 + \frac{1}{2} \phi_R^2 + \frac{1}{2} \phi_I^2 + |\eta|^2. \tag{31}$$

From the above, it is clear that the scalar portal coupling $\lambda_{H\phi}$ is the only connection between the dark and SM sectors. It allows h to couple to $|\eta|^2$, $\phi_{R,I}^2$, as well as ζ^2 , and leads to the mixing between h and ζ , with mass-squared matrix given by

$$\mathcal{M}_{h\zeta}^2 = \begin{pmatrix} 2\lambda_H v_H^2 & 2\lambda_{H\phi} v_H v_D \\ 2\lambda_{H\phi} v_H v_D & 2\lambda_D v_D^2 \end{pmatrix}. \tag{32}$$

This mixing also implies that the dark gauge bosons $X_{1,2,3}$ are also coupled to the SM through $\lambda_{H\phi}$.

The $\lambda_{H\phi}$ coupling allows the $Z_3 \times Z_2$ dark matter to scatter off nucleons through the SM Higgs boson. It is required to be very small, of order 10^{-4} , to agree with present experimental data. However, it should also be big enough so that the physical scalar which is mostly ζ could decay rapidly through its small h component to SM particles. For the purpose of

discussing the relic abundance, the role of $\lambda_{H\phi}$ can remain sub-dominant, as in our previous study [5]. Under the residual dark $Z_3 \times Z_2$ symmetry, the SM particles as well as ζ and X_3 do not transform, whereas

$$\eta \sim (\omega, +), \quad \phi_{R,I} \sim (1, -), \quad (X_1 - iX_2)/\sqrt{2} \sim (\omega, -). \quad (33)$$

This means that there are at least two stable dark-matter components. We will assume that η is the lightest, and ϕ_I the second lightest, with both annihilating to ζ . We choose our input parameters to be

$$g_D, v_D, x, \lambda_{H\phi}, M_\zeta, M_\eta, M_{\phi_I},$$

with the mass hierarchy

$$M_{\phi_R} > M_{X_3} > M_{X_{1,2}} > M_{\phi_I} > M_\eta > M_\zeta. \quad (34)$$

Since the dark sector particles except ζ decays within the dark sector itself, it is also possible to have three-component DM by choosing a compressed mass spectrum, as studied in [13] in the context of $U(1)_X \rightarrow Z_3 \times Z_2$ dark matter. Unlike this work containing several scalar fields and hence more free parameters, we have very limited number of free parameters due to the presence of only one scalar multiplet responsible for dark $SU(2)$ gauge symmetry breaking and resulting DM phenomenology. We discuss the details of two-component DM phenomenology in the upcoming section.

III. DARK MATTER PHENOMENOLOGY

As mentioned above, we have a natural two-component DM model due to the residual $Z_3 \times Z_2$ discrete symmetry from the spontaneous breaking of dark gauge $SU(2)$ by a Higgs quadruplet. To discuss the relic density of two-component dark matter [14–18] quantitatively, we first write the coupled Boltzmann equations (BEs) for comoving number densities of the

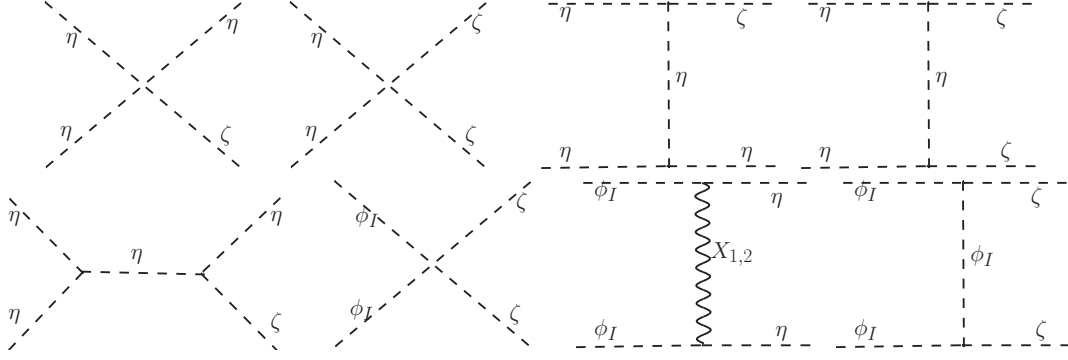


FIG. 1: Dominant Semi-annihilation and annihilation channels for DM components η and ϕ_I .

two DM candidates which we assume to be η and ϕ_I respectively. We have assumed that η is the lightest Z_3 odd particle in the spectrum and is absolutely stable. On the other hand, due to the unbroken Z_2 symmetry, ϕ_I is also stable along with η . In Fig. 1, we show the dominant Feynman diagrams contributing to the annihilation and semi-annihilation processes of both η and ϕ_I . Since ϕ_I is neutral under Z_3 it gives rise to typical annihilation channels into lighter particles while η , being charged under Z_3 , also has semi-annihilation processes like $\eta\eta \rightarrow \eta\zeta$, typical of Z_3 dark matter. We have assumed that $X_{1,2,3}$, ϕ_R are heavier and hence these final states will not contribute to the relic density calculation. Also, as mentioned earlier, the Higgs portal coupling $\lambda_{H\phi}$ is assumed to be small so that the annihilation processes to SM final states remain sub-dominant. However, this coupling cannot be arbitrarily small as the dark sector gets thermalised with the SM by virtue of Higgs portal interactions only. This leads to a lower bound on $\lambda_{H\phi}$ from the requirement of dark sector thermalisation. Considering the point-like interaction $\zeta\zeta \rightarrow hh$ with a cross-section $\sigma \approx \lambda_{H\phi}^2/(32\pi s)$, one can find the lower bound on $\lambda_{H\phi}$ by demanding the rate of interaction to be greater than the Hubble expansion rate at some high-temperature T . This leads to $n^{\text{eq}}\langle\sigma v\rangle(T) > \mathbf{H}(T) = 1.66\sqrt{g_*}T^2/M_{\text{Pl}}$. Demanding the dark sector to thermalise with the SM above the TeV scale ($T \geq 1\text{ TeV}$) leads to $\lambda_{H\phi} \gtrsim 10^{-7}$. Choosing it to be very small, however, can lead to very early DM-SM decoupling. This requires the tracking of dark sector temperature evolution till the epoch of

dark sector freeze-out. In this work, we consider $\lambda_{H\phi}$ to be in the ballpark of $10^{-4} - 10^{-3}$ and assume the dark sector and the SM baths to evolve with a common temperature.

Choosing the variable to be $x_i = (M_i/T)$ with $i = 1, 2$ for η, ϕ_I respectively, the BEs in the limit of two stable dark matter candidates with the possible annihilations specified above, can be written as

$$\begin{aligned} \frac{dY_\eta}{dx_1} = \frac{\beta s}{\mathbf{H}x_1} & \left(-\langle\sigma(\eta\eta \rightarrow \text{SM SM})v_{\text{rel}}\rangle [Y_\eta^2 - (Y_\eta^{\text{eq}})^2] - \langle\sigma(\eta\eta \rightarrow \zeta\zeta)v_{\text{rel}}\rangle [Y_\eta^2 - (Y_\eta^{\text{eq}})^2] \right. \\ & - \langle\sigma(\eta\eta \rightarrow \eta h)v_{\text{rel}}\rangle [Y_\eta^2 - Y_\eta^{\text{eq}}Y_\eta] - \langle\sigma(\eta\eta \rightarrow \eta\zeta)v_{\text{rel}}\rangle [Y_\eta^2 - Y_\eta^{\text{eq}}Y_\eta] \\ & \left. + \langle\sigma(\phi_I\phi_I \rightarrow \eta\eta)v_{\text{rel}}\rangle \left[Y_{\phi_I}^2 - \frac{(Y_{\phi_I}^{\text{eq}})^2}{(Y_\eta^{\text{eq}})^2} Y_\eta^2 \right] \right), \end{aligned} \quad (35)$$

$$\begin{aligned} \frac{dY_{\phi_I}}{dx_2} = \frac{\beta s}{\mathbf{H}x_2} & \left(-\langle\sigma(\phi_I\phi_I \rightarrow \text{SM SM})v_{\text{rel}}\rangle [Y_{\phi_I}^2 - (Y_{\phi_I}^{\text{eq}})^2] - \langle\sigma(\phi_I\phi_I \rightarrow \zeta\zeta)v_{\text{rel}}\rangle [Y_{\phi_I}^2 - (Y_{\phi_I}^{\text{eq}})^2] \right. \\ & \left. - \langle\sigma(\phi_I\phi_I \rightarrow \eta\eta)v_{\text{rel}}\rangle \left[Y_{\phi_I}^2 - \frac{(Y_{\phi_I}^{\text{eq}})^2}{(Y_\eta^{\text{eq}})^2} Y_\eta^2 \right] \right), \end{aligned} \quad (36)$$

where $Y_x = (n_x/s)$ denotes comoving number density for $x \equiv \eta, \phi_I$ with

$$\beta(T) = 1 + \frac{1}{3} \frac{T}{g_s(T)} \frac{dg_s(T)}{dT}$$

and \mathbf{H} being the Hubble parameter. The first term of the right hand side of Eq. (35) shows the annihilation to the SM final states whereas the second, third and fourth terms show the annihilation to $\zeta\zeta$, semi-annihilation to Higgs and ζ respectively. The last term represents the conversion processes between the two dark matter particles. Similarly, the first term of the right hand side of Eq. (36) is for the annihilation to the SM final states and the second and the third terms are for the annihilation to ζ and conversion to η respectively. Among all these processes the two ζ final state and the semi-annihilation processes give the dominant contribution to the relic density due to the chosen mass hierarchy as well as small Higgs portal interactions. In order to calculate the thermally averaged annihilation cross-sections and solve the above BEs numerically, we use `micrOMEGAs` [19].

Let us discuss the numerical results of the model. As discussed above, we have two different components of stable dark matter in this scenario, the lightest Z_3 -charged particle η and the lightest Z_2 -odd particle ϕ_I . However, in this study we have restricted ourselves to the regime where M_η is smaller than M_{ϕ_I} . For our analysis, we have considered the mixing between the dark sector and the SM to be small governed by the smallness of $\lambda_{H\phi}$ which is also motivated by the direct detection constrain from various direct detection experiments. We consider the two DM masses to be free parameters with $M_\eta < M_{\phi_I}$. We also choose the remaining free parameters $g_D, v_D, x, \lambda_{H\phi}, M_\zeta$ in a way which maintains the dark sector mass hierarchy in Eq. (34). In Fig. 2, we have shown the total DM relic density as function of M_η for three different benchmark values of M_ζ . One can note that total relic density decreases with decreasing mass splitting between M_η and M_ζ . For a fixed value of M_η , as we increase M_ζ in order to decrease the mass splitting $M_\eta - M_\zeta$, it increases the scalar interactions of η as seen from Eq. (29) enhancing its annihilation rate thereby decreasing the relic abundance. Due to such dependence of scalar couplings on M_ζ , $\eta\eta \rightarrow \eta\zeta$ and $\eta\eta \rightarrow \zeta\zeta$ processes dominate the relic abundance. Notably, for the chosen mass hierarchy of $X_{1,2}, \phi_R, \eta$, the total DM relic is dominated by η as strong annihilation and conversion rates of heavier DM candidate ϕ_I reduce its relative abundance. In order to make it clear, we scan the parameter space for the chosen hierarchy. In the left panel of Fig. 3, we have shown the allowed parameter space in $M_\eta - M_\zeta$ plane from the observed total relic density constraints of dark matter. The right panel of the same figure shows the allowed parameter space in $M_\eta - M_{\phi_I}$ plane. Color bar in the left panel shows the variation of the gauge coupling g_D whereas the color bar in the right panel shows the variation of relative relic abundance of η ($R_\eta = \Omega_\eta/(\Omega_\eta + \Omega_{\phi_I})$). As seen from the right panel plot, the total relic density is dominated by η for the chosen mass hierarchy. This is due to large annihilation rate of ϕ_I by virtue of its large coupling with ζ for the chosen mass spectrum of different scalars, as seen from the scalar interactions in Eq. (29). Apart from the large annihilation rate, we have also set M_{ϕ_I} to be heavier than

M_η which gives more Boltzmann suppression in the number density of ϕ_I . This can be seen that ϕ_I contributes nearly 5% of the total relic abundance when $M_{\phi_I} \sim M_\eta$. In Fig. 4, we have shown the variation of effective scalar couplings $\lambda_{\eta\eta\eta\zeta}, \lambda_{\eta\eta\zeta\zeta}$ as a function of g_D where the color bar represents the variation of M_η . These couplings are not free parameters and as shown in Eq. (29), they depend upon other parameters as

$$\lambda_{\eta\eta\eta\zeta} = \frac{1}{3\sqrt{6}} \left(\frac{2M_{\phi_R}^2}{v_D^2} - \frac{3M_\eta^2}{v_D^2} \right), \quad \lambda_{\eta\eta\zeta\zeta} = \frac{1}{4} \left(\frac{M_\zeta^2}{2v_D^2} + \frac{M_\eta^2}{v_D^2} \right). \quad (37)$$

The correlations between g_D , M_η and the quartic couplings shown in Fig. 4 can be understood as follows. Increasing g_D increases the $\lambda_{\eta\eta\eta\zeta}$ and $\lambda_{\eta\eta\zeta\zeta}$ as shown in the figure and this also increases the annihilation cross section of η . However, this was compensated by increasing M_η as for point interactions $\sigma \sim \frac{\lambda^2}{8\pi M_\eta^2}$. Similar correlation can also be seen between g_D and M_η in Fig. 3.

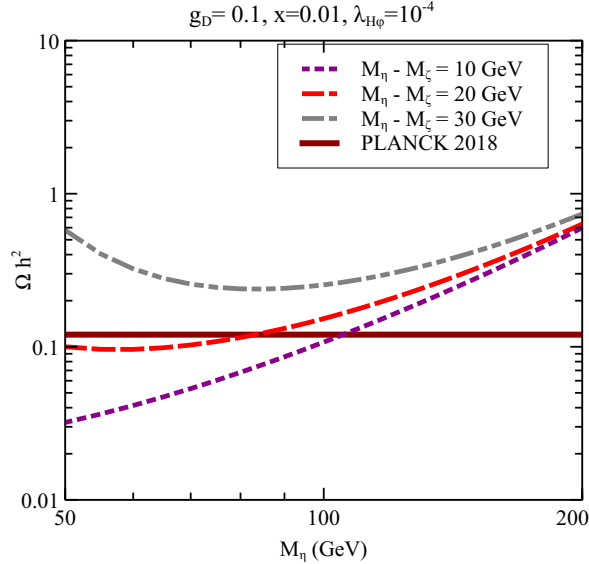


FIG. 2: Total relic density of dark matter as a function of M_η for three different mass splitting between M_η and M_ζ .

We have chosen Higgs portal coupling $\lambda_{H\phi} = 10^{-4}$ in the above analysis, which is sufficient to bring dark sector in thermal equilibrium with the SM while keeping the direct detection

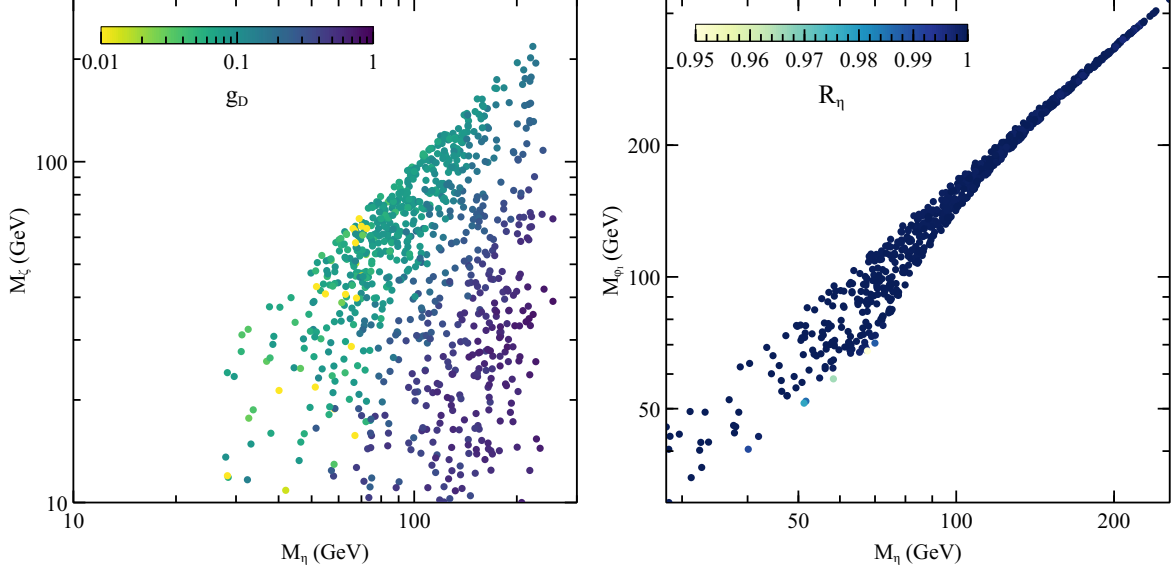


FIG. 3: Left panel: Allowed parameter space in $M_\eta - M_\zeta$ plane from total DM relic abundance criteria. Right panel: Allowed parameter space in $M_\eta - M_{\phi_I}$ plane from total DM relic abundance criteria. Color bar in the left (right) panel shows the variation of dark gauge coupling g_D (relative relic abundance of η given by $R_\eta = \Omega_\eta / (\Omega_\eta + \Omega_{\phi_I})$).

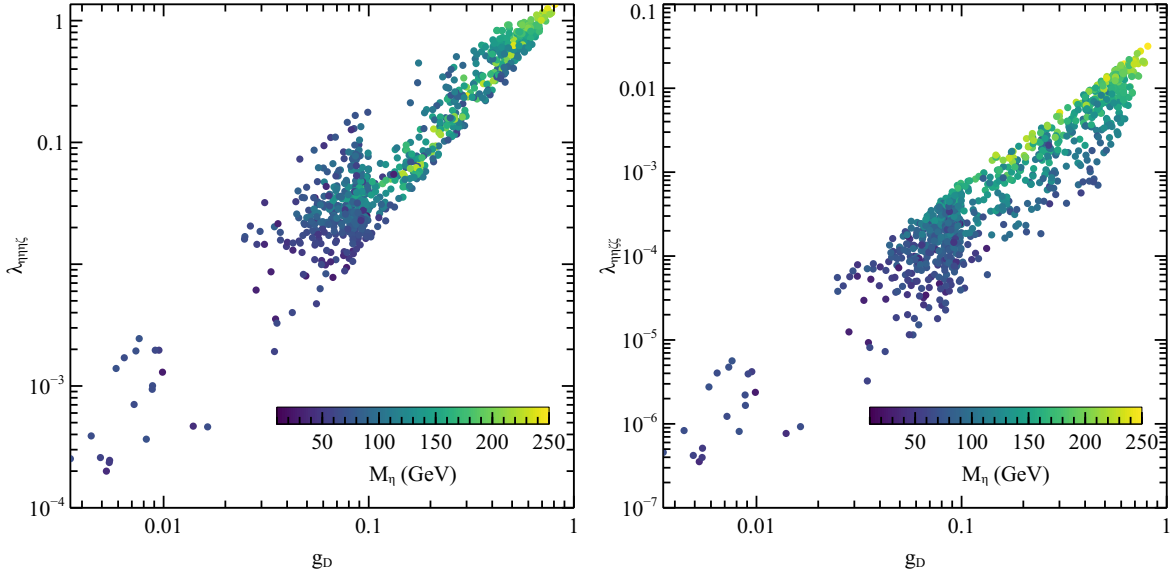


FIG. 4: Allowed parameter space in $g_D - \lambda_{\eta\eta\zeta}$ plane (Left panel) and in $g_D - \lambda_{\eta\eta\zeta\zeta}$ plane from total DM relic abundance criteria.

cross-section suppressed. For higher values of Higgs portal coupling, this model can also be

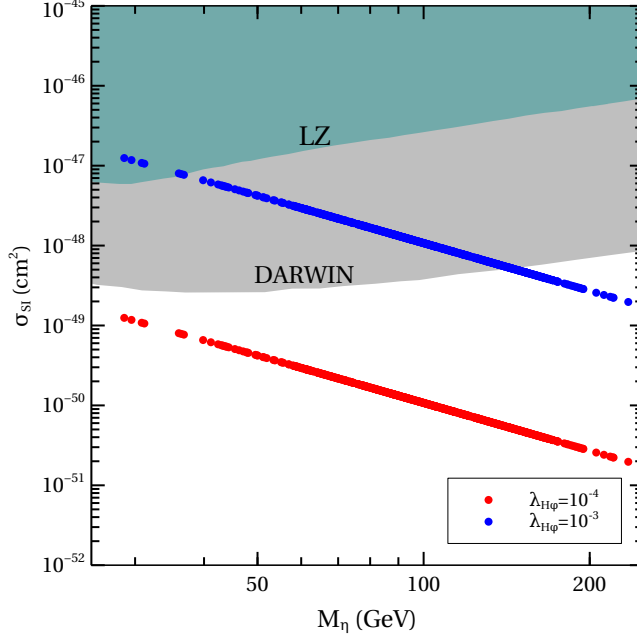


FIG. 5: Spin-independent direct detection cross-section as a function of DM mass for two different values of Higgs portal coupling $\lambda_{H\phi}$.

tested in the ongoing and future direct detection experiments [20, 21]. Due to Higgs portal interactions, dominant DM component namely, η can scatter off nucleon at tree level leading to spin-independent DM-nucleon scattering cross-section tightly constrained by experiments. In Fig. 5, we show the spin-independent DM-nucleon cross-section as a function of M_η . The current constraint from LZ [20] and future sensitivity of DARWIN [21] are shown as shaded regions. The points corresponding to $\lambda_{H\phi} = 10^{-4}$ correspond to the data points shown in Fig. 3. Clearly, they remain even out of reach at future experiments. We check that a larger Higgs portal coupling $\lambda_{H\phi} = 10^{-3}$ which is still small enough not to alter the relic density analysis discussed above, can bring the direct detection rate within current and future experimental reach for certain range of DM masses, keeping the model verifiable. Semi-annihilating DM can also have interesting indirect detection signatures [22].

IV. CONCLUSION

We have studied a gauge $SU(2)$ symmetry as the origin of dark matter where a scalar quadruplet plays the role of breaking the gauge symmetry spontaneously into a residual $Z_3 \times Z_2$ symmetry responsible for stabilising dark matter. This framework not only gives rise to a fundamental origin of Z_3 dark matter, but also predicts a second DM candidate, stabilised by a Z_2 symmetry. In this setup, ϕ_I , the DM matter component stabilised due to the unbroken Z_2 symmetry, will always be heavier than the Z_3 DM candidate η (following Eq. (28)). This also leads to conversion from ϕ_I to η . As a result, the relic density will always be dominated by the lighter Z_3 charged component of DM η . We have studied the thermal scalar DM scenario considering the dark sector to reach thermal equilibrium with the standard model by virtue of Higgs portal couplings. Dark matter relic abundance is primarily governed by interactions within the dark sector like annihilation, semi-annihilation and conversions with the annihilation into SM particles being sub-dominant due to small Higgs portal couplings required to obey direct detection constraints. Suitable choices of Higgs portal couplings can lead to observable direct detection cross-section keeping the model verifiable. While we have assumed specific mass hierarchy among dark sector particles to study the phenomenology of two scalar DM candidates, other possible mass hierarchies can lead to mixed type of DM consisting of both dark scalar and dark gauge bosons. One can always make η to be lighter than the dark gauge bosons ($X_{1,2}$) which are also charged under Z_3 symmetry and make them the stable DM candidates. Phenomenology of such dark gauge boson DM has been studied in [5]. In addition to the possibilities of different thermal DM candidates, one can also have different relic generation mechanism depending upon the relative magnitude of Higgs portal coupling $\lambda_{H\phi}$ and dark sector couplings like g_D . For example, if $\lambda_{H\phi}$ is very small but dark sector couplings are sizeable, dark sector may evolve with a different temperature leading to dark freeze-out [23]. We leave such detailed

studies to future works.

Acknowledgments

This work was supported in part by the U. S. Department of Energy Grant No. DE-SC0008541. The work of DN is supported by National Research Foundation of Korea (NRF)'s grants with grants No. NRF-2019R1A2C3005009(DN). The work of DB is supported by SERB, Government of India grant MTR/2022/000575.

-
- [1] B.-L. Young, Front. Phys. (Beijing) **12**, 121201 (2017), [Erratum: Front.Phys.(Beijing) 12, 121202 (2017)].
 - [2] E. Ma, Phys. Rev. Lett. **115**, 011801 (2015), 1502.02200.
 - [3] E. Ma, Phys. Lett. B **809**, 135736 (2020), 1912.11950.
 - [4] T. Hambye, JHEP **01**, 028 (2009), 0811.0172.
 - [5] D. Borah, E. Ma, and D. Nanda, Phys. Lett. B **835**, 137539 (2022), 2204.13205.
 - [6] E. Ma, LHEP **02**, 01 (2018), 1804.00374.
 - [7] G. Etesi, J. Math. Phys. **37**, 1596 (1996), hep-th/9706029.
 - [8] A. Adulpravitchai, A. Blum, and M. Lindner, JHEP **09**, 018 (2009), 0907.2332.
 - [9] K. Agashe and G. Servant, Phys. Rev. Lett. **93**, 231805 (2004), hep-ph/0403143.
 - [10] E. Ma, Phys. Lett. B **662**, 49 (2008), 0708.3371.
 - [11] B. Batell, Phys. Rev. D **83**, 035006 (2011), 1007.0045.
 - [12] S. F. King and Y.-L. Zhou, JHEP **11**, 173 (2018), 1809.10292.
 - [13] S.-M. Choi, J. Kim, P. Ko, and J. Li, JHEP **09**, 028 (2021), 2103.05956.
 - [14] Q.-H. Cao, E. Ma, J. Wudka, and C. P. Yuan (2007), 0711.3881.
 - [15] K. M. Zurek, Phys. Rev. **D79**, 115002 (2009), 0811.4429.
 - [16] Z.-P. Liu, Y.-L. Wu, and Y.-F. Zhou, Eur. Phys. J. C **71**, 1749 (2011), 1101.4148.
 - [17] G. Belanger and J.-C. Park, JCAP **1203**, 038 (2012), 1112.4491.
 - [18] A. Adulpravitchai, B. Batell, and J. Pradler, Phys. Lett. B **700**, 207 (2011), 1103.3053.
 - [19] G. Bélanger, F. Boudjema, A. Pukhov, and A. Semenov, Comput. Phys. Commun. **192**, 322 (2015), 1407.6129.
 - [20] J. Aalbers et al. (LUX-ZEPLIN) (2022), 2207.03764.

- [21] J. Aalbers et al. (DARWIN), JCAP **11**, 017 (2016), 1606.07001.
- [22] G. Arcadi, F. S. Queiroz, and C. Siqueira, Phys. Lett. B **775**, 196 (2017), 1706.02336.
- [23] J. L. Feng, H. Tu, and H.-B. Yu, JCAP **10**, 043 (2008), 0808.2318.